

Bifurcations analysis of turbulent energy cascade

Nicola de Divitiis

"La Sapienza" University, Dipartimento di Ingegneria Meccanica e Aerospaziale, Via Eudossiana, 18, 00184 Rome, Italy

Abstract

This note studies the mechanism of turbulent energy cascade through an opportune bifurcations analysis of the Navier–Stokes equations, and furnishes explanations on the more significant characteristics of the turbulence. A statistical bifurcations property of the Navier–Stokes equations in fully developed turbulence is proposed, and a spatial representation of the bifurcations is presented, which is based on a proper definition of the fixed points of the velocity field. The analysis first shows that the local deformation can be much more rapid than the fluid state variables, then explains the mechanism of energy cascade through the aforementioned property of the bifurcations, and gives reasonable argumentation of the fact that the bifurcations cascade can be expressed in terms of length scales. Furthermore, the study analyzes the characteristic length scales at the transition through global properties of the bifurcations, and estimates the order of magnitude of the critical Taylor–scale Reynolds number and the number of bifurcations at the onset of turbulence.

Keywords:

Energy cascade, Bifurcations, Fixed points, Lyapunov theory.

1. Introduction

The main aim of this work is to analyze the turbulent mechanism of energy cascade by means of the bifurcations properties of the Navier–Stokes equations. This analysis is accomplished in the case of incompressible fluid in an infinite domain. Moreover, through this analysis, we want to corroborate the basic hypotheses of previous works (de Divitiis (2011, 2014)) where the finite–scale Lyapunov theory is used to describe the homogeneous isotropic turbulence. There, the theory, which leads to the closure of von Kármán & Howarth (1938) and Corrsin (1951) equations, is also based on the assumption that the bifurcations cascade law can be expressed in terms of length scales, and on the hypothesis that the relative kinematics between two contiguous particles is much faster than the fluid state variables. This latter is justified by the fact that in turbulence the kinematics of fluid deformation exhibits chaotic behavior and huge mixing (Ottino (1989, 1990)), and allows to express velocity and temperature fluctuations with Navier–Stokes and temperature equations, through the local fluid deformation (de Divitiis (2011, 2014)).

The study first introduces the bifurcations of the Navier–Stokes equations (NS–bifurcations), in line with the classical theory of differential equations (Ruelle & Takens (1971); Eckmann (1981)) and shows that the local fluid deformation $\partial\mathbf{x}/\partial\mathbf{x}_0$ can be much more rapid than the fluid state variables. The phenomenon of energy cascade is then studied through a statistical property of the Navier–Stokes equations in regimes of fully developed chaos. This property, which represents an important element of this work, is obtained through basic characteristics of the bifurcations in developed chaos, and gives the link between NS–bifurcations and energy cascade mechanism.

Next, to found the link between length scales and NS–bifurcations, the fixed points of the velocity field and the corresponding bifurcations (u–bifurcations) are properly defined. According to this definition, these u–bifurcations are shown to be non–material moving points which represent the trace of the NS–bifurcations in the fluid domain. Such spatial representation justifies the fact that the bifurcations cascade can be expressed in terms of length scales. This representation, together to general properties of the route toward the chaos and to the fractal characteristics of the bifurcations in developed turbulence, allows to analytically express one reasonable bifurcations cascade law in terms of length scales.

Through these elements, we furnish plausible argumentations that the NS–bifurcations are responsible for the main properties of turbulence, such as the chaotic fluid motion, the energy cascade, the continuous distribution of the length scales.

Moreover, a relationship between the order of magnitude of R_λ^* and N is found, where R_λ^* and N are, respectively, the critical Taylor–scale Reynolds number and number of bifurcations at the transition. This estimation, based on adequate hypotheses about the length scales, gives $N = 3$ and $R_\lambda^* = 4 \div 14$, in agreement with the several theoretical and experimental sources of the literature. Next, R_λ^* is also estimated beginning from the fully developed isotropic turbulence using the closed von Kármán–Howarth equation proposed by de Divitiis (2011). The two procedures give results in agreement with each other.

2. Background: Bifurcations of Navier–Stokes equations

This section recalls some of the elements of the Navier–Stokes equations and the general properties of the bifurcations which are necessary for the purposes of the present analysis.

The dimensionless Navier–Stokes equations are

$$\begin{aligned} \nabla \cdot \mathbf{u} &= 0, \\ \frac{\partial \mathbf{u}}{\partial t} &= -\mathbf{u} \cdot \nabla \mathbf{u} - \nabla p + \frac{1}{Re} \nabla^2 \mathbf{u} \end{aligned} \quad (1)$$

where $Re = UL/\nu$ is the Reynolds number, $\mathbf{u}=\mathbf{u}(\mathbf{x}, t)$ and $p=p(\mathbf{x}, t)$ are dimensionless velocity and pressure, whereas U and L are the reference velocity and length. For sake of convenience, the momentum Navier–Stokes equations are formally written by eliminating the pressure field in Eqs. (1) through the continuity equation

$$\dot{\mathbf{u}} = \mathbf{N}(\mathbf{u}; Re) \equiv \mathbf{N}_0(\mathbf{u}) + \frac{1}{Re} \mathbf{L}\mathbf{u} \quad (2)$$

where $\dot{\mathbf{u}}$ is the Eulerian time derivatives of the velocity field,

$$\mathbf{N} : \{\mathbf{u}\} \rightarrow \left\{ \frac{\partial \mathbf{u}}{\partial t} \right\} \quad (3)$$

is the nonlinear operator representing the R.H.S. of the momentum Navier–Stokes equations, and $\{\mathbf{u}\}$ and $\{\partial \mathbf{u}/\partial t\}$ are the sets of \mathbf{u} and $\partial \mathbf{u}/\partial t$, respectively. In Eq. (2), $\mathbf{N}_0(\mathbf{u})$ is the nonlinear quadratic operator representing the inertia and pressure forces, whereas the linear operator $\mathbf{L}\mathbf{u}$ gives the viscosity term. In the case of homogeneous fluid in infinite domain, if $\mathbf{u}(\mathbf{x}, t)$ is a solution of Eq. (2), then $\mathbf{u}(\mathbf{x} + \mathbf{h}, t)$ satisfies Eq. (2), where \mathbf{h} is an arbitrary displacement, i.e.

$$\dot{\mathbf{u}}(\mathbf{x}, t) = \mathbf{N}(\mathbf{u}(\mathbf{x}, t); Re) \Rightarrow \dot{\mathbf{u}}(\mathbf{x} + \mathbf{h}, t) = \mathbf{N}(\mathbf{u}(\mathbf{x} + \mathbf{h}, t); Re), \quad \forall \mathbf{h} \quad (4)$$

In line with Ruelle & Takens (1971), we suppose that $\{\mathbf{u}\}$ can be replaced by a finite-dimensional manifold, thus Eq. (2) is here analyzed through the classical theory of the differential equations. Now, to define the bifurcations of the Navier–Stokes equations, consider the steady solutions of Eq. (2)

$$\mathbf{N}(\mathbf{u}; Re) = 0 \quad (5)$$

If $Re = Re_0$ is properly small, the unique steady solution $\mathbf{u}(Re_0) = \mathbf{u}(\mathbf{x}; Re_0)$ is calculated by inversion of Eq. (5), and for $Re > Re_0$, the steady solutions $\mathbf{u}(Re)$ can be obtained starting from $\mathbf{u}(Re_0)$, by applying the implicit function theorem to Eq. (5)

$$\mathbf{u}(Re) = \mathbf{u}(Re_0) - \int_{Re_0}^{Re} \nabla_{\mathbf{u}} \mathbf{N}^{-1} \frac{\partial \mathbf{N}}{\partial Re} dRe \quad (6)$$

where $\nabla_{\mathbf{u}} \mathbf{N} \equiv \partial \mathbf{N}(\mathbf{u}; Re)/\partial \mathbf{u}$ is the Jacobian of \mathbf{N} with respect to \mathbf{u} . The velocity field $\mathbf{u}(Re)$ can be determined with Eq. (6) as long as $\nabla_{\mathbf{u}} \mathbf{N}$ is nonsingular, i.e. when the determinant $\det(\nabla_{\mathbf{u}} \mathbf{N}) \neq 0$.

The bifurcations of the Navier–Stokes equations occur when $\nabla_{\mathbf{u}}\mathbf{N}$ exhibits at least an eigenvalue with zero real part (NS–bifurcations). There, $\det(\nabla_{\mathbf{u}}\mathbf{N}) = 0$ thus, following Eq. (6), $\mathbf{u}(Re)$ can degenerate in two or more solutions. As the consequence of the structure of Eq. (2), we have the following route toward the chaos: For small Re , the viscosity forces are stronger than the inertia ones and \mathbf{N} behaves like a linear operator with $\det(\nabla_{\mathbf{u}}\mathbf{N}) \neq 0$. When the Reynolds number increases, as long as $\nabla_{\mathbf{u}}\mathbf{N}$ is nonsingular, $\partial\mathbf{u}/\partial Re$ exhibits smooth variations, whereas at a certain Re , this Jacobian becomes singular and $\partial\mathbf{u}/\partial Re$ appears to be discontinuous with respect to Re . Of course, the route toward the turbulence can be of different kinds, such as, for example, those described by Ruelle & Takens (1971), Feigenbaum (1978), and by Pomeau & Manneville (1980). In general, the chaotic motion is observed when the number of encountered bifurcations is about greater than three. Figure 1 reports a qualitative scheme of the

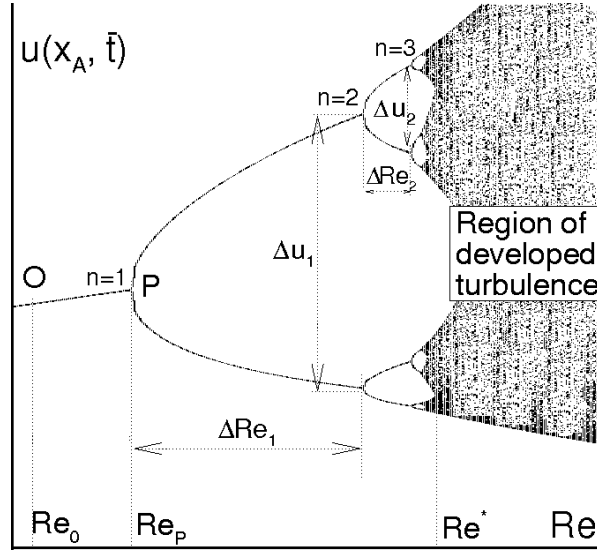


Figure 1: Qualitative scheme of NS–bifurcations.

bifurcations tree, in which one component of $\mathbf{u}(\mathbf{x}_A, \bar{t})$ is shown in function of Re , where \mathbf{x}_A and \bar{t} are assigned position and time. Starting from Re_0 , the diagram is regular, until Re_p , where the first bifurcation determines two branches. Increasing again Re , other bifurcations occur. In the figure, Δu denotes the distance between two branches which born from the same bifurcation, ΔRe represents the distance between two successive bifurcations and n is the number of the encountered bifurcations starting from Re_0 .

If the Reynolds number does not exceed its critical value value, say Re^* , the velocity fields satisfying Eq. (6) are limited in number, thus also n is moderate, and the branches corresponds to the intermediate stages of the route toward the chaos.

Conversely, when $Re > Re^*$, we have the region of developed turbulence. There, $\lambda_{NS} > 0$, where λ_{NS} is the maximal Lyapunov exponent of the Navier–Stokes equations, formally calculated as

$$\lambda_{NS} = \lim_{T \rightarrow \infty} \frac{1}{T} \int_0^T \frac{\mathbf{y} \cdot \nabla_{\mathbf{u}}\mathbf{N}\mathbf{y}}{\mathbf{y} \cdot \mathbf{y}} dt, \quad (7)$$

$$\dot{\mathbf{y}} = \nabla_{\mathbf{u}}\mathbf{N}(\mathbf{u}; Re)\mathbf{y},$$

$$\dot{\mathbf{u}} = \mathbf{N}(\mathbf{u}; Re),$$

and \mathbf{y} is the Lyapunov vector of the Navier–Stokes equations. Accordingly, Re^* depends on \mathbf{u} , and is defined as the minimum value of the Reynolds number at which $\lambda_{NS} \geq 0$. For $Re > Re^*$, the diverse velocity fields satisfying Eq. (6), determine an extended complex geometry made by several points whose minimum distance is very small. There, the equation $\mathbf{N}(\mathbf{u}, Re) = 0$ is satisfied in a huge number of points of $\{\mathbf{u}\}$ which are very close with each other, whereas $\mathbf{N}(\mathbf{u}, Re) \neq 0$ elsewhere. This corresponds to a situation in which \mathbf{u} , \mathbf{N} and $\nabla_{\mathbf{u}}\mathbf{N}$ exhibit abrupt variations.

It is worth to remark two general properties of the bifurcation diagrams. 1) The first property regards the overall dimension along u of the bifurcations tree: following such property, this dimension varies quite regularly with respect to Re also through the transition, and can be represented by one proper smooth rising function of Re of class $C^0(Re)$. 2) The other property pertains the beginning of chaos: the region of developed turbulence is bounded at the onset of turbulence by bifurcations lines which separate the region of the developed chaos by the remaining zone. These lines form bifurcation tongues, regions of developed chaos, whose local extension along Δu increases with Re until to overlap with each other.

The Bifurcations are also responsible for the sharp variations of the characteristic length scales of the velocity fields. For $Re \ll Re^*$, the solutions of Eq. (5) can be expressed by Fourier series of a given characteristic length scale. When Re steadily rises, each encountered bifurcation introduces new solutions whose characteristic scales are independent from the previous ones until to reach the edge of turbulence where $Re \lesssim Re^*$. These are independent scales discretely distributed. Thereafter, for $Re \gtrsim Re^*$, such discrete distribution disappears, and the scales seem to be continuously distributed.

3. Bifurcation of unsteady solutions and divergence of phase trajectories

In the case of unsteady flow, the bifurcations are responsible for multiple unsteady velocity fields. In fact, during the motion, multiple solutions $\hat{\mathbf{u}}$ can be determined, at each instant, through inversion of Eq. (2)

$$\begin{aligned}\dot{\mathbf{u}} &= \mathbf{N}(\mathbf{u}; Re) \\ \hat{\mathbf{u}}(Re) &= \mathbf{N}^{-1}(\dot{\mathbf{u}}; Re)\end{aligned}\tag{8}$$

If $Re \ll Re^*$, \mathbf{N} behaves like a linear operator, and Eq. (8) gives $\hat{\mathbf{u}} \equiv \mathbf{u}(\mathbf{x}, t)$ as unique solution, whereas if Re is properly high, \mathbf{N}^{-1} is a multivalued operator and Eq. (8) determines several velocity fields $\hat{\mathbf{u}}$. That is, the current velocity field $\mathbf{u}(\mathbf{x}, t)$ corresponds to several other solutions $\hat{\mathbf{u}}(\mathbf{x}, t; Re)$ which give the same field $\dot{\mathbf{u}}(\mathbf{x}, t)$. For $Re > Re^*$ a huge number of these solutions are unstable, thus the bifurcations determine a situation where $\mathbf{u}(\mathbf{x}, t)$ tends to sweep the entire velocity field set, accordingly the motion is expected to be chaotic with a high level of mixing.

When Re is given, a single NS–bifurcation corresponds to several trajectories bifurcations in the hodograph space and to a growth of the velocity gradient $\nabla_{\mathbf{x}}\mathbf{u}$. To show this, consider now the two velocity fields $\mathbf{u} = \mathbf{u}(\mathbf{x}, t)$ and $\mathbf{u}'(\mathbf{x}, t) = \mathbf{u}(\mathbf{x} + \mathbf{r}, t)$, where \mathbf{r} , and $\boldsymbol{\xi} = \mathbf{u}' - \mathbf{u}$. Thanks to the property (4) (homogeneous fluid in infinite space), \mathbf{u} and \mathbf{u}' are both solutions of Eq. (2), thus the evolution equations of $\boldsymbol{\xi}$ coincide with those of perturbation of the velocity field, and if $r = |\mathbf{r}|$ is quite small, these equations are

$$\begin{aligned}\dot{\boldsymbol{\xi}} &= \nabla_{\mathbf{u}}\mathbf{N} \boldsymbol{\xi}, \\ \dot{\mathbf{u}} &= \mathbf{N}(\mathbf{u}; Re)\end{aligned}\tag{9}$$

Hence, the classical theory of the differential equations can be applied to Eq. (9). For sake of simplicity, we suppose that at the onset of the motion all the eigenvalues of $\nabla_{\mathbf{u}}\mathbf{N}(\mathbf{u}, Re)$ exhibit negative real part, and that the NS–bifurcation happens for $t = t^* > 0$. There, at least an eigenvalue of $\nabla_{\mathbf{u}}\mathbf{N}(\mathbf{u}, Re)$ crosses the imaginary axis, and the phase trajectories, initially contiguous, thereafter diverge. Figure 2 shows three pairs of trajectories in the same hodograph plane (u_x, u_y), each representing the velocity components in the pairs of points $(\mathbf{x}_1, \mathbf{x}_1 + \mathbf{r})$, $(\mathbf{x}_2, \mathbf{x}_2 + \mathbf{r})$ and $(\mathbf{x}_3, \mathbf{x}_3 + \mathbf{r})$, where the arrows denote increasing time. Continuous and dashed lines represent the velocities calculated in $\mathbf{x}_1, \mathbf{x}_2, \mathbf{x}_3$ and $\mathbf{x}_1 + \mathbf{r}, \mathbf{x}_2 + \mathbf{r}, \mathbf{x}_3 + \mathbf{r}$, respectively, whereas the points $\mathbf{B}_1, \mathbf{B}_2, \mathbf{B}_3$ give the velocities at $t = t^*$, thus these are the image of the NS–bifurcation in the hodograph plane. After the NS–bifurcation $\boldsymbol{\xi}_1(t), \boldsymbol{\xi}_2(t)$ and $\boldsymbol{\xi}_3(t)$ diverge, and this means that a bifurcation causes the lost of informations with respect to the initial condition $\boldsymbol{\xi}_1(0), \boldsymbol{\xi}_2(0)$ and $\boldsymbol{\xi}_3(0)$. In particular, for what concerns the single trajectory $\mathbf{2}-\mathbf{B}_2$, after \mathbf{B}_2 it degenerates in the two branches $\mathbf{B}_2 - \mathbf{C}$ and $\mathbf{B}_2 - \mathbf{D}$ which represent two possible phase trajectories, thus $\partial\mathbf{u}/\partial t = 0$ in \mathbf{B}_2 . After \mathbf{B}_2 , Eq. (9) does not indicate which of the branches the fluid will choose, thus very small variations on the initial condition or little perturbations, are of paramount importance for the choice of the branch that the fluid will follow (Prigogine (1994)).

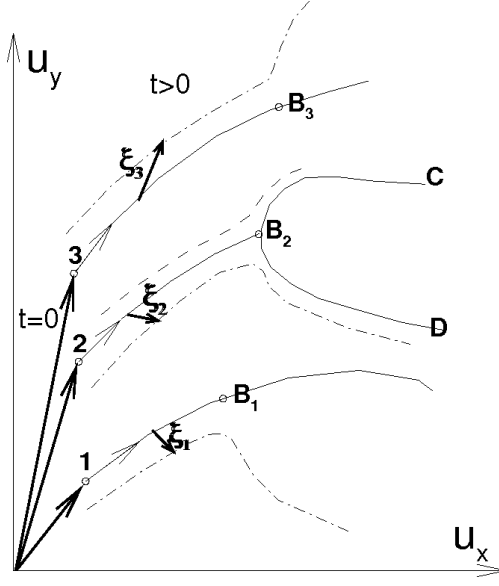


Figure 2: Qualitative scheme of phase trajectories in the hodograph plane of three different points of the space.

4. Property of the local fluid deformation in developed turbulence

This section presents reasonable argumentations that, in turbulence, the local fluid deformation

$$\frac{\partial \mathbf{x}}{\partial \mathbf{x}_0} \quad (10)$$

can be much more rapid than the fluid state variables, where \mathbf{x}_0 and \mathbf{x} are material coordinates, and the function $\chi : \mathbf{x}_0 \rightarrow \mathbf{x}$ gives the current position \mathbf{x} of a fluid particle located at the referential position \mathbf{x}_0 at $t = t_0$. To show this, observe that, in Eq. (9), ξ corresponds to variations of the velocity gradient $\nabla_{\mathbf{x}} \mathbf{u}$ which thus changes according to

$$\nabla_{\mathbf{x}} \mathbf{u}(\mathbf{x}, t) = \exp\left(\int_0^t \nabla_{\mathbf{u}} \mathbf{N} dt\right) \nabla_{\mathbf{x}} \mathbf{u}(\mathbf{x}, 0) \quad (11)$$

where the exponential denotes the series expansion of operators

$$\exp\left(\int_0^t \nabla_{\mathbf{u}} \mathbf{N} dt\right) = \mathbf{I} + \int_0^t \nabla_{\mathbf{u}} \mathbf{N} dt + \dots \quad (12)$$

$\nabla_{\mathbf{x}} \mathbf{u}(\mathbf{x}, 0)$ is the initial condition, and \mathbf{I} is the identity map. The bifurcations determine abrupt changing in $\nabla_{\mathbf{u}} \mathbf{N}$ which in turn produces important increments of the velocity gradient according to Eq. (11). Although such variations are very significant and $\lambda_{NS} > 0$, due to the viscosity, $\nabla_{\mathbf{x}} \mathbf{u}$ is however a function of slow growth of $t \in (t_0, \infty)$.

On the contrary, $\partial \mathbf{x} / \partial \mathbf{x}_0$ is not bounded by the dissipation effects. This deformation, related to the relative kinematics between two contiguous particles, is represented by the infinitesimal separation vector $d\mathbf{x}$ between the particles, which varies according to

$$d\dot{\mathbf{x}} = \nabla_{\mathbf{x}} \mathbf{u} d\mathbf{x} \quad (13)$$

The Lyapunov analysis of this equation gives the local deformation in terms of the maximal Lyapunov exponent $\Lambda = \max(\Lambda_1, \Lambda_2, \Lambda_3)$ associated to Eq. (13)

$$\frac{\partial \mathbf{x}}{\partial \mathbf{x}_0} \approx e^{\Lambda(t-t_0)} \quad (14)$$

where Λ_1 , Λ_2 and Λ_3 are the Lyapunov exponents of Eq. (13). Due to the fluid incompressibility $\Lambda > 0$, and as $\|\nabla_{\mathbf{x}}\mathbf{u}\| \gg 0$, the exponent $\Lambda \approx \|\nabla_{\mathbf{x}}\mathbf{u}\|$ is expected to be high, thus according to Eq. (14) $\partial\mathbf{x}/\partial\mathbf{x}_0$ can be much faster than $\nabla_{\mathbf{x}}\mathbf{u}$ and \mathbf{u} . Therefore, as the local fluid deformation is not bounded by the viscosity, $\partial\mathbf{x}/\partial\mathbf{x}_0$ is represented by functions of exponential growth, whereas the fluid state variables are functions of slow growth of $t \in (t_0, \infty)$.

Remark. This property can have implications for what concerns the basic formulation for deriving the Navier–Stokes equations. In fact, momentum and continuity equations are derived from an integral formulation of balance equations by means of the Green theorem, and this latter can be applied to regions which exhibit smooth boundaries during the motion (Truesdell (1977) and references therein). Now, if $\partial\mathbf{x}/\partial\mathbf{x}_0$ is much more rapid than \mathbf{u} and exhibits abrupt spatial variations, the boundaries of fluid region become irregular in very short times, and this implies that the Navier–Stokes equations could require the consideration of very small scales and times for describing the fluid motion.

5. Relationship bifurcations–energy cascade in fully developed turbulence

The purpose of this section is to show the link between the bifurcations and the phenomenon of turbulent energy cascade. To study this, a simple statistical property of the Navier–Stokes equations in the regime of fully developed chaos is proposed. This property, arising from basic elements of the bifurcations, is here applied to the Navier–Stokes equations in the form (2). To this end, consider now Fig. 3, where a scheme of two contiguous phase trajectories in the hodograph plane is shown in proximity of the trajectory bifurcation \mathbf{B} . These trajectories correspond to velocity

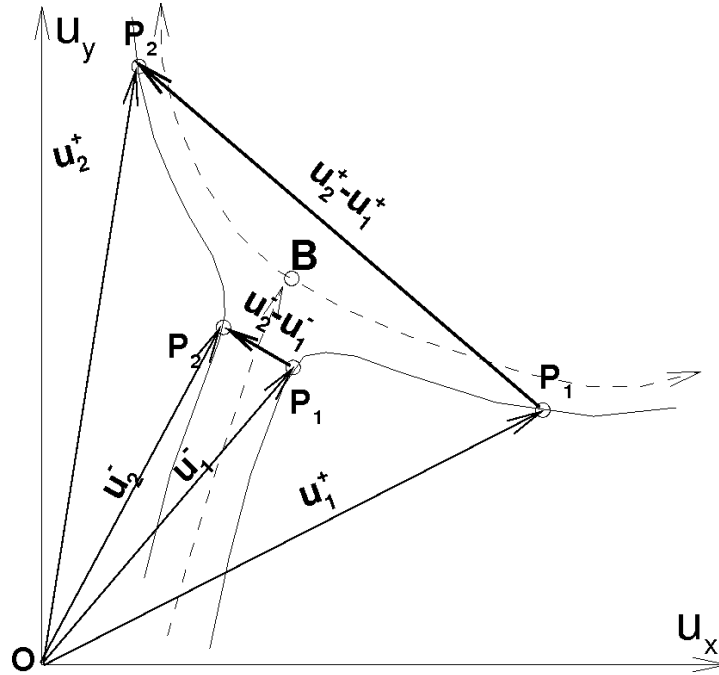


Figure 3: Scheme of the velocities variations near a bifurcation in the hodograph plane.

variations in two assigned points \mathbf{x}_1 and $\mathbf{x}_2 = \mathbf{x}_1 + \mathbf{r}$, where $r = |\mathbf{r}| > 0$ is arbitrarily small. The figure shows the velocity arrows P_1 and P_2 which describe the two phase trajectories, initially close with each other, that thereafter diverge because of the bifurcation. Let t^- and t^+ instants for which both P_1 and P_2 approach to \mathbf{B} and move away from it, respectively. In developed turbulence, $\lambda_{NS} > 0$, and the phase trajectories diverge, i.e.

$$|\mathbf{u}_2^+ - \mathbf{u}_1^+| \gg |\mathbf{u}_2^- - \mathbf{u}_1^-| \quad (15)$$

moreover thanks to the numerous bifurcations $\det(\nabla_{\mathbf{u}}\mathbf{N}) \approx 0$, therefore we expect that

$$|\mathbf{u}_1^+| \approx |\mathbf{u}_1^-|, \quad |\mathbf{u}_2^+| \approx |\mathbf{u}_2^-| \quad (16)$$

The inequality (15) and Eq. (16) imply that

$$\mathbf{u}_1^+ \cdot (\mathbf{u}_2^+ - \mathbf{u}_1^+) \ll \mathbf{u}_1^- \cdot (\mathbf{u}_2^- - \mathbf{u}_1^-) \quad (17)$$

The condition (17) is frequently satisfied in the chaotic regime, whereas the opposite inequality is possible but not probable. Hence, from the statistical point of view, it is reasonable that

$$\frac{\partial}{\partial t} \langle \mathbf{u} \cdot (\mathbf{u}' - \mathbf{u}) \rangle \leq 0, \quad \forall r \text{ small} \quad (18)$$

where $\mathbf{u} = \mathbf{u}_1$, $\mathbf{u}' = \mathbf{u}_2$, and $\langle \cdot \rangle$ denotes the average over the velocity ensemble. Moreover, for relatively high values of r , due to the numerous trajectory bifurcations in between \mathbf{x}_1 and \mathbf{x}_2 , the inequality (17) will be satisfied in average, thus we assume that

$$\int_V \frac{\partial}{\partial t} \langle \mathbf{u} \cdot (\mathbf{u}' - \mathbf{u}) \rangle dV' \leq 0, \quad \forall V, \quad (19)$$

in which $dV' = dr_x dr_y dr_z$ is the elemental volume with $d\mathbf{r} = (dr_x, dr_y, dr_z)$, and $\int_V dV' = 4/3\pi r^3$. Taking into account Eq. (2), Eqs. (19) and (18) are both summarized by the following condition

$$\int_V \langle \mathbf{N} \cdot \Delta \mathbf{u} + \mathbf{u} \cdot \Delta \mathbf{N} \rangle dV' \leq 0, \quad \forall V \quad (20)$$

where $\mathbf{N} = \mathbf{N}_1$, $\Delta \mathbf{N} = \mathbf{N}' - \mathbf{N}_1$, and $\Delta \mathbf{u} = \mathbf{u}' - \mathbf{u}$. Observe that Eq. (20) has been obtained from Eq. (2), for arbitrary $Re > Re^*$. Due to this arbitrarily and considering that the bifurcations are caused by the nonlinear terms of the Navier–Stokes equations, we obtain

$$\int_V \langle \mathbf{N}_0 \cdot \Delta \mathbf{u} + \mathbf{u} \cdot \Delta \mathbf{N}_0 \rangle dV' \leq 0, \quad \forall V \quad (21)$$

Equation (21) represents the proposed relationship, which expresses the influence of the bifurcations on the fluid motion.

At this stage of the analysis, we argue that the bifurcations determine the transfer of kinetic energy from large to small scales. To demonstrate this, we will show, starting from Eq. (21), that

$$H_3(r) < 0 \quad \forall r \geq 0, \quad (22)$$

$$\lim_{r \rightarrow \infty} H_3(r) = 0$$

in the case of homogeneous isotropic turbulence, where $H_3(r)$ is the third dimensionless statistical moment (skewness) of the longitudinal component of $\mathbf{u}' - \mathbf{u}$. This is shown by means of the evolution equation of the velocity correlation. This equation is obtained through the Navier–Stokes equations written in two points \mathbf{x} and $\mathbf{x}' = \mathbf{x} + \mathbf{r}$, taking into account that, in such condition $\langle \mathbf{N}_0 \mathbf{u} \rangle \equiv 0$ (von Kármán & Howarth (1938))

$$\frac{\partial}{\partial t} \langle \mathbf{u} \cdot \mathbf{u}' \rangle = Re^{-1} (2 \langle \mathbf{u} \cdot \mathbf{L} \mathbf{u} \rangle + \langle \mathbf{L} \mathbf{u} \cdot \Delta \mathbf{u} + \mathbf{L} \Delta \mathbf{u} \cdot \mathbf{u} \rangle) \quad (23)$$

$$+ \langle \mathbf{N}_0 \cdot \Delta \mathbf{u} + \Delta \mathbf{N}_0 \cdot \mathbf{u} \rangle$$

The first integral of Eq. (23) is the von Kármán & Howarth (1938) equation, the evolution equation of the longitudinal velocity correlation function. First and second terms at the R.H.S. of Eq. (23) give respectively, the rate of

kinetic energy and the spatial variations of the velocity correlation due to the viscosity, whereas the third one, arising from the inertia forces, is responsible for the mechanism of energy cascade and identifies the term with $H_3(r)$ (von Kármán & Howarth (1938))

$$\langle \mathbf{N}_0 \cdot \Delta \mathbf{u} + \Delta \mathbf{N}_0 \cdot \mathbf{u} \rangle = \nabla \cdot \langle (\mathbf{u} \cdot \mathbf{u}')(\mathbf{u} - \mathbf{u}') \rangle \quad (24)$$

where

$$\langle \mathbf{N}_0 \cdot \Delta \mathbf{u} + \mathbf{u} \cdot \Delta \mathbf{N}_0 \rangle = 0 \quad \text{for } r = 0, \quad (25)$$

and

$$\lim_{r \rightarrow \infty} \langle \mathbf{N}_0 \cdot \Delta \mathbf{u} + \mathbf{u} \cdot \Delta \mathbf{N}_0 \rangle = 0, \quad (26)$$

Following Eq. (25) the bifurcations do not modify the average kinetic energy rate, thus they are only responsible for the energy cascade, whereas Eq. (26) states that their effect vanishes for $r \rightarrow \infty$.

Now, in line with von Kármán & Howarth (1938)

$$\frac{1}{r^2} \frac{\partial}{\partial r} (r^3 K(r)) \equiv \nabla \cdot \langle (\mathbf{u} \cdot \mathbf{u}')(\mathbf{u} - \mathbf{u}') \rangle \quad (27)$$

where $K(r)$ is an even function of r directly related to the longitudinal triple correlation function $k(r) = \langle u_r^2 u_r' \rangle / u^3$, according to

$$\frac{1}{r^4} \frac{\partial}{\partial r} (r^4 k(r)) = \frac{K(r)}{u^3} \quad (28)$$

where $u = \sqrt{\langle u_r^2 \rangle} \equiv \sqrt{\langle \mathbf{u} \cdot \mathbf{u} \rangle / 3}$, $u_r = \mathbf{u} \cdot \mathbf{r} / r$ and k is an odd function of r which vanishes for $r \rightarrow \infty$ and such that $k = O(r^3)$ near the origin (von Kármán & Howarth (1938)). Now, integrating Eq. (27) with respect to the volume V and taking into account Eq. (21) and that $K(0) = 0$, we have $K(r) < 0 \forall r > 0$, where due to isotropy, $dV' = dr_x dr_y dr_z = 4\pi r^2 dr$. Integrating again Eq. (28) with $k(0) = 0$, we obtain $k(r) < 0 \forall r > 0$. Accordingly, the skewness of Δu_r and of $\partial u_r / \partial r$ are both negative

$$H_3(r) = \frac{\langle (\Delta u_r)^3 \rangle}{\langle (\Delta u_r)^2 \rangle^{3/2}} \equiv \frac{6k(r)}{(2(1 - f(r)))^{3/2}} < 0, \quad \forall r > 0, \quad (29)$$

$$H_3(0) = \lim_{r \rightarrow 0} H_3(r) = \frac{k'''(0)}{(-f''(0))^{3/2}} < 0$$

where $f = \langle u_r u_r' \rangle / u^2$ is the longitudinal correlation function, and the superscript Roman numerals denote derivatives with respect to r . As $\nabla \cdot \langle (\mathbf{u} \cdot \mathbf{u}')(\mathbf{u} - \mathbf{u}') \rangle = O(r^2)$ near the origin (von Kármán & Howarth (1938)), $H_3(0) < 0$ assumes finite value, and since $\lim_{r \rightarrow \infty} f = \lim_{r \rightarrow \infty} k = 0$, then $\lim_{r \rightarrow \infty} H_3(r) = 0$.

In conclusion, the proposed property of the bifurcations (21) implies the phenomenon of kinetic energy cascade and that the bifurcations are the driving force of turbulence.

6. Fixed points and bifurcations of velocity fields

The NS-bifurcations exhibit implications for what concerns the characteristic scales of the velocity field. To analyze this link, the fixed points associated to the current velocity field $\mathbf{u}(\mathbf{x}, t) \in C^1(\{\mathbf{x}\} \times \{t\})$ are first introduced. These fixed points are here defined as the points \mathbf{X} satisfying

$$\hat{\mathbf{u}}(\mathbf{X}; Re) = 0, \quad (30)$$

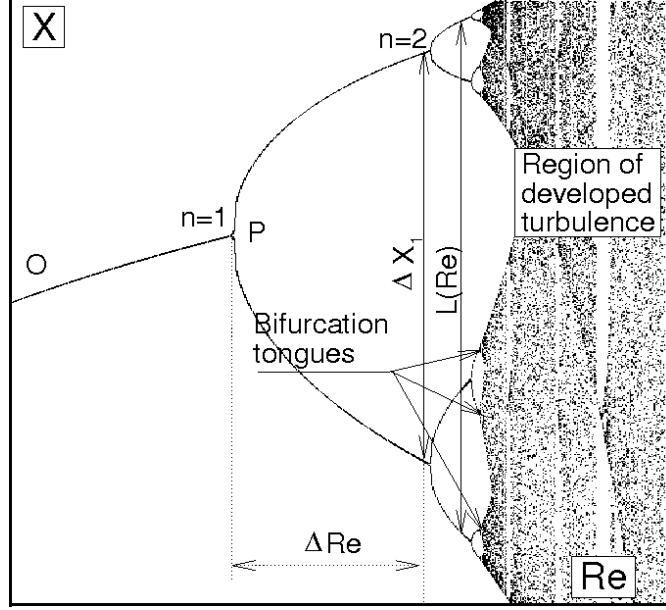


Figure 4: Qualitative scheme of bifurcations of a given velocity field.

where $\hat{\mathbf{u}}(\mathbf{X}; Re)$ is calculated with Eq. (8). To study these points, we recall that $\mathbf{u}(\mathbf{x}, t)$ determines $\hat{\mathbf{u}}(\mathbf{x}; Re) = \mathbf{N}^{-1}(\hat{\mathbf{u}}; Re)$ which is not unique and depends on the Reynolds number. Thus, these points also depend on Re , and if $\mathbf{X}(Re_0)$ represents the fixed points calculated at $Re_0 \ll Re^*$, $\mathbf{X}(Re)$ can be formally obtained with the implicit function theorem

$$\mathbf{X}(Re) = \mathbf{X}(Re_0) + \int_{Re_0}^{Re} \nabla_{\mathbf{x}} \hat{\mathbf{u}}^{-1} \nabla_{\mathbf{u}} \mathbf{N}^{-1} \frac{\partial \mathbf{N}}{\partial Re} dRe \quad (31)$$

where $Re > Re_0$. $\mathbf{X}(Re)$ can be determined with Eq. (31) if $\det(\nabla_{\mathbf{u}} \mathbf{N} \nabla_{\mathbf{x}} \hat{\mathbf{u}}) \neq 0$. If we exclude the cases where $\det \nabla_{\mathbf{x}} \hat{\mathbf{u}} = 0$, the u-bifurcations are defined as those fixed points where the operator $\nabla_{\mathbf{u}} \mathbf{N}$ admits at least one eigenvalue with zero real part. Hence, the u-bifurcations are the image of the NS-bifurcations in the fluid domain, and the previous considerations concerning the route toward the chaos can be applied to Eq. (31). For unsteady flow, the fixed points continuously vary with the time. Figure 4 shows the situation corresponding to unsteady velocity fields at a given instant \bar{t} , where ΔX is the bifurcation scale, a characteristic length which expresses the distance between branches which born from the same bifurcation.

These u-bifurcations determine sizable variations on the characteristic scales of the velocity field. If, for $Re \ll Re^*$, the velocity field is represented by the Fourier series of a given basic scale, one bifurcation corresponds to new solutions $\hat{\mathbf{u}}$ whose Fourier characteristic lengths, about proportional to ΔX , are independent from the previous one. Therefore, each bifurcation adds new independent scales, and, after the transition, the several characteristic lengths are continuously distributed, thus \mathbf{u} is there represented by the Fourier transform.

Returning to Eq. (31), the diagram of Fig.4 is qualitatively similar to that of Fig. 1, therefore it exhibits the same general properties: 1) $L(Re)$ smoothly varies with respect to Re , where $L(Re)$ is the overall dimension of the bifurcation tree along X . In particular, we assume that $L(Re)$ is a rising function of Re with $L(Re) \in C^0(Re)$. 2) existence of bifurcations tongues whose width increases with Re , and that thereafter are overlapped.

Another important property is that, for $Re < Re^*$, the bifurcations are limited in number, and the sum of the distances between contiguous branches does not exceed $L(Re)$ (Mandelbrot (2002); Mainzer (2005))

$$\sum_{n \neq 1} \Delta X_n < \Delta X_1 - \Delta X_N < L(Re) \quad (32)$$

Vice versa, for $Re > Re^*$, the bifurcations frequently happen, the bifurcations tree will exhibit fractional dimension and self-similarity (Mandelbrot (2002); Mainzer (2005)), while the distance between the successive u-

bifurcations is very small. Accordingly, we have

$$\sum_{n \neq 1} \Delta X_n > L(Re) > \Delta X_1 \quad (33)$$

This equation expresses the well known property that the perimeter \mathcal{P} of one fractal geometry is much greater than its overall dimension as $\mathcal{P} \approx A^{D/2}$ and $L(Re) \approx A^{1/2}$, where A is the area of the fractal object and D is its fractal dimension (see for instance Mandelbrot (2002) and references therein).

Hence, immediately before the transition ($Re \lesssim Re^*$), the situation is characterized by a distribution of discrete scales ΔX_n , whereas for $Re > Re^*$, the bifurcations behave like continuous transitions and ΔX plays the role of a real variable.

7. Bifurcations cascade in terms of length scales

The length scales vary with time and their average values are expressed in function of n . Figure 5 (Right) qualitatively shows l_n immediately before the transition ($Re \lesssim Re^*$, filled symbols), where N is the number of encountered bifurcations at Re^* . These scales, discretely distributed, are expressed by the succession

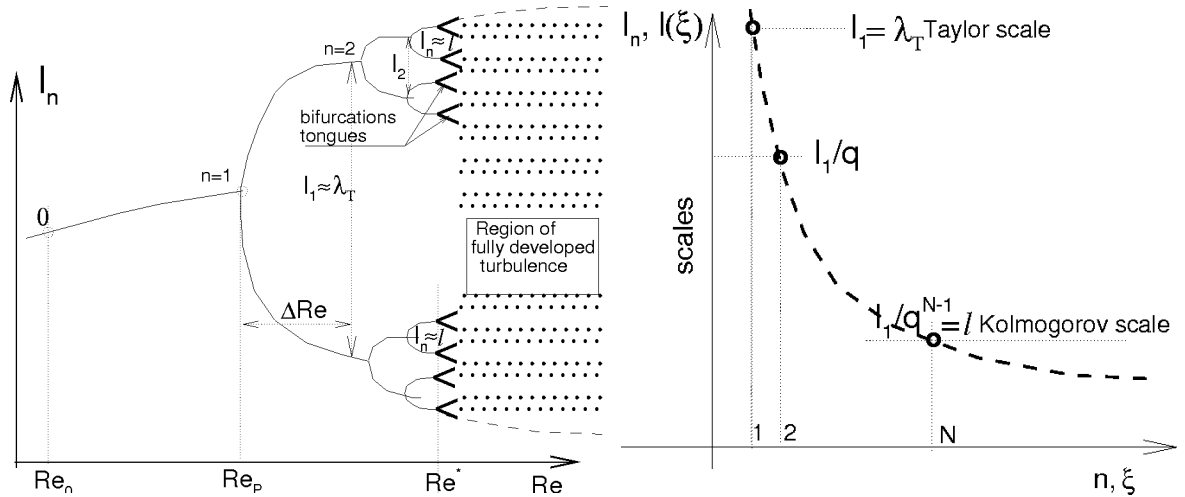


Figure 5: Left: Schematic of the bifurcations cascade law in terms of length scales. Right: Discrete (Filled symbols) and continuous (dashed line) length scales distribution for $Re \approx Re^*$

$$\{l_n, n = 1, 2, \dots, N\} \quad (34)$$

Conversely, to represent the continuous scales l in developed turbulence, l is in terms of $\xi > 0$, a real variable which replaces n in developed turbulence. Hence

$$l = l(\xi), \quad \xi \in \mathbb{R}^+ \quad (35)$$

where $l(\xi) d\xi$ represents the elemental scale in developed turbulence.

As discussed in sect. 6, for $Re \gtrsim Re^*$, the lengths describe a dense set which includes the characteristic scales before the transition. Accordingly, the function $l(\xi)$ is chosen in such a way that

$$l(n) = l_n, \quad n = 1, 2, \dots, N \quad (36)$$

Next, because of the aforementioned self-similarity (Mandelbrot (1967, 2002)), l_n and $l(\xi)$ are supposed to be, respectively, a geometric progression and an exponential function, i.e.

$$l_n = \frac{l_1}{q^{n-1}}, \quad n = 1, 2, \dots, N, \quad \text{for } Re \lesssim Re^* \quad (37)$$

$$l(\xi) = \frac{l_1}{q^{\xi-1}}, \quad \xi \in \mathbb{R}^+, \quad \text{for } Re \gtrsim Re^*$$

where $q > 1$.

Now, in order to obtain an estimate of q , observe that following the inequality (32), the sum of the distances ΔX_n does not exceed $\Delta X_1 - \Delta X_N$, for $Re \lesssim Re^*$, i.e.

$$\sum_{n=2}^N l_n < l_1 - l_N \equiv l_1 \left(1 - \frac{1}{q^{N-1}}\right) \quad (38)$$

On the contrary, for $Re > Re^*$, thanks to the fractal properties of the bifurcations, the sum of such these distances is much greater than $L(Re)$ (Mandelbrot (2002), see ineq. (33)), and this can be expressed taking into account that $\xi \in \mathbb{R}^+$

$$\int_1^\infty l(\xi) d\xi > l_1 \quad (39)$$

As $\{l_n, n = 1, 2, \dots\}$ is a geometric succession, the inequality (38) is satisfied for $q > 2$ and N arbitrary, whereas the condition (39) is satisfied for $q < e$, that is

$$2 < q < e \quad (40)$$

8. Estimation of the critical Taylor-scale Reynolds number

In fully developed turbulence, the Taylor-scale Reynolds number is defined by

$$R_\lambda = \frac{u\lambda_T}{\nu} \quad (41)$$

where $\lambda_T = 1/\sqrt{-f'''(0)}$ is the Taylor scale. R_λ , λ_T and u are linked by means of the relation (Batchelor (1953))

$$\frac{\lambda_T}{\ell} = 15^{1/4} \sqrt{R_\lambda}, \quad (42)$$

where ℓ is the Kolmogorov microscale.

The critical Taylor-scale Reynolds number R_λ^* is first estimated starting from the route toward the chaos, using the bifurcations cascade seen at the previous section, and assuming opportune properties of the length scales. Thereafter, R_λ^* is also estimated beginning from the fully developed isotropic turbulence, adopting the closure equation presented in de Divitiis (2011) for the von Kármán–Howarth equation, and a plausible condition for λ_T .

8.1. Estimation of R_λ^* through the route toward the chaos

To estimate R_λ^* through the route toward the turbulence, the relationship between R_λ^* and N is searched. Now, to obtain this link, observe that, due to the presence of the bifurcation tongues, the Kolmogorov scale ℓ can not exceed $l(N)$ at the onset of turbulence. At the same time, $L(Re) \approx \lambda_T$ for $Re > Re^*$, and thanks to the smooth variations of

Table 1: Critical Taylor–scale Reynolds number calculated for $N = 2, 3$, and 4 , for different values of q .

q	$Re_\lambda^*(N=2)$	$Re_\lambda^*(N=3)$	$Re_\lambda^*(N=4)$
2.000	1.03	4.13	16.52
2.250	1.31	6.62	33.50
$\alpha \approx 2.503$	1.62	10.13	63.49
$e \approx 2.718$	1.91	14.10	104.16

$L(Re)$ through the transition (see Fig. 5 (Left)), λ_T can not be less than $l(1)$, thus $\ell < l(n) < \lambda_T$ for $Re \approx Re^*$. Hence, according to Eq. (37), we assume that

$$l(n) = \frac{\lambda_T}{q^{n-1}}, \quad \ell = \frac{\lambda_T}{q^{N-1}} \quad (43)$$

Combining Eqs. (43) and (42), we obtain

$$R_\lambda^* = \frac{q^{2N-2}}{\sqrt{15}} \quad (44)$$

which expresses the searched relationship. With reference to table 1, all the values of R_λ^* calculated for $N = 2$ and $q \in [2, e]$ are of the order of the unity and this is not compatible with λ_T which represents the correlation scale, while the values $R_\lambda^* = 4 \div 14$ obtained for $N = 3$ and $q \in [2, e]$ are acceptable. In particular, if q is assumed to be equal to the second Feigenbaum constant ($\alpha = 2.502\dots$), $R_\lambda^* \approx 10$. For $N = 4$, all the values of R_λ^* seem to be quite high in comparison with a plausible minimum values of R_λ , especially for high values of q .

These orders of magnitude of R_λ^* calculated for $N = 3$, agree with the different theoretical routes to the turbulence (Ruelle & Takens (1971); Feigenbaum (1978); Pomeau & Manneville (1980); Eckmann (1981)), and with the diverse experimental data (Gollub & Swinney (1975); Giglio et al (1981); Libchaber & Maurer (1979)) which state that the transition occurs when $N \gtrsim 3$.

8.2. Estimation of R_λ^* through the fully developed turbulence

Next, to estimate R_λ^* starting from the regime of fully developed homogeneous isotropic turbulence, the solutions of the von Kármán–Howarth equation are analyzed in function of R_λ . To determine R_λ^* , we need an auxiliary condition which defines the lower limit for the existence of this regime of turbulence. To found this condition, observe that the homogeneous isotropic turbulence is an unsteady regime, where u and λ_T change with t according to (von Kármán & Howarth (1938); Batchelor (1953))

$$\frac{du^2}{dt} = -\frac{10u^2\nu}{\lambda_T^2} \quad (45)$$

$$\frac{5\nu}{\lambda_T^4} + \frac{1}{\lambda_T^3} \frac{d\lambda_T}{dt} = \frac{7}{6}uk^{III}(0) + \frac{7}{3}\nu f^{IV}(0) \quad (46)$$

where Eqs. (45) and (46) are the equations for the coefficients of the powers r^0 and r^2 , respectively, of the von Kármán–Howarth equation. The term responsible for the energy cascade is the first one at the R.H.S. of Eq. (46), whereas the second one is due to the viscosity. According to Eq. (46), if the energy cascade is sufficiently stronger than the viscosity effects, then $d\lambda_T/dt < 0$. Hence, a reasonable condition to estimate R_λ^* can consist in to search the value of R_λ for which

$$\frac{d\lambda_T}{dt} = 0 \quad (47)$$

at a given instant. This value of R_λ^* depends on the adopted closure equation for K . If we use the results of the Lyapunov theory proposed by de Divitiis (2011), K is in terms of f and $\partial f/\partial r$

$$K = u^3 \sqrt{\frac{1-f}{2}} \frac{\partial f}{\partial r} \quad (48)$$

thus Eq. (47) is satisfied for (Batchelor (1953))

$$R_\lambda \equiv R_\lambda^* = 2 \left(\frac{7}{3} \varphi - 5 \right) \text{ where } \varphi = \frac{f^{IV}(0)}{(f^{II}(0))^2} \quad (49)$$

Following such estimation, R_λ^* is related to the behavior of f near the origin through $\varphi > 15/7$. For instance, when f is a gaussian function

$$f = \exp\left(f^{II}(0) \frac{r^2}{2}\right), \text{ then } \varphi = 3, \quad R_\lambda^* = 4. \quad (50)$$

whereas if, according to the Kolmogorov law, f behaves like

$$f \approx 1 - cr^{2/3}, \quad c > 0, \text{ then } \varphi = 4.8, \quad R_\lambda^* = 12.4. \quad (51)$$

where $f^I(\lambda_T/\sqrt{2})$ and $f^{II}(\lambda_T/\sqrt{2})$ are assumed to be equal to the corresponding derivatives of $1 + 1/2 f_0^{II} r^2 + 1/4! f_0^{IV} r^4$ in $r = \lambda_T/\sqrt{2}$. These values are in qualitatively good agreement with those of the previous analysis based on the bifurcations.

9. Conclusion

We conclude this work by observing that the proposed properties of fully developed turbulence based on bifurcations explain the energy cascade phenomenon in agreement with the literature, and motivate the fact that the local fluid strain can be much faster than the fluid state variables. Furthermore, the spatial representation of the bifurcations justifies that the bifurcations cascade can be expressed in terms of length scales, and allows to argue that the scales are continuously distributed in developed turbulence. The fractal properties of the bifurcations and the proposed link between the characteristic scales through the transition lead to a relationship between critical Reynolds number and number of bifurcations at the transition, resulting $N=3$ and $R_\lambda^* \approx 4 \div 14$ in line with the literature. R_λ^* is also estimated as that value of the Taylor-scale Reynolds number at which $d\lambda_T/dt = 0$ in the isotropic turbulence. The two procedures provide values of R_λ^* in agreement with each other.

10. Acknowledgments

This work was partially supported by the Italian Ministry for the Universities and Scientific and Technological Research (MIUR).

References

- BATCHELOR, G.K., *The Theory of Homogeneous Turbulence*. Cambridge University Press, Cambridge, 1953.
- CORRSIN S., The Decay of Isotropic Temperature Fluctuations in an Isotropic Turbulence, *Journal of Aeronautical Science*, **18**, pp. 417–423, no. 12, 1951.
- DE DIVITIIS, N., Lyapunov Analysis for Fully Developed Homogeneous Isotropic Turbulence, *Theoretical and Computational Fluid Dynamics*, DOI: 10.1007/s00162-010-0211-9.
- DE DIVITIIS, N., Finite Scale Lyapunov Analysis of Temperature Fluctuations in Homogeneous Isotropic Turbulence, *Appl. Math. Modell.*, DOI: 10.1016/j.apm.2014.04.016.

- ECKMANN, J.P., Roads to turbulence in dissipative dynamical systems *Rev. Mod. Phys.* **53**, 643–654, 1981.
- FEIGENBAUM, M. J., *J. Stat. Phys.* **19**, 1978.
- GIGLIO M., MUSAZZI S., PERINI U., Transition to chaotic behavior via a reproducible sequence of period doubling bifurcations, *Phys. Rev. Lett.* **47**, 243, 1981.
- GOLLUB, J.P., SWINNEY, H.L., Onset of Turbulence in a Rotating Fluid., *Phys. Rev. Lett.* **35**, 927, 1975.
- VON KÁRMÁN, T., HOWARTH, L., On the Statistical Theory of Isotropic Turbulence., *Proc. Roy. Soc. A*, **164**, 14, 192, 1938.
- MAINZER, K., *Symmetry And Complexity: The Spirit And Beauty Of Nonlinear Science*, World Scientific, 2005.
- MANDELBROT B. B., How Long Is the Coast of Britain? Statistical Self-Similarity and Fractional Dimension, *Science*, **156**, 636–638, 1967, doi:10.1126/science.156.3775.636.
- MANDELBROT, B. B., *Gaussian Self-Affinity and Fractals: Globality, The Earth, 1/f Noise, and R/S*, Springer, 2002.
- MAURER, J., LIBCHABER A., Rayleigh–Bénard Experiment in Liquid Helium: Frequency Locking and the onset of turbulence, *Journal de Physique Letters* **40**, L419–L423, 1979.
- OTTINO, J. M. *The kinematics of mixing: stretching, chaos, and transport*, Cambridge Texts in Applied Mathematics, New York, 1989.
- OTTINO, J. M., Mixing, Chaotic Advection, and Turbulence., *Annu. Rev. Fluid Mech.* **22**, 207–253, 1990.
- POMEAU, Y., MANNEVILLE, P., *Commun Math. Phys.* **74**, 189, 1980.
- PRIGOGINE, I., *Time, Chaos and the Laws of Chaos*. Ed. Progress, Moscow, 1994.
- RUELLE, D., TAKENS, F., *Commun. Math Phys.* **20**, 167, 1971.
- TRUESDELL, C. *A First Course in Rational Continuum Mechanics*, Academic, New York, 1977.